CHALMERS | UNIVERSITY OF GOTHENBURG

PREPRINT 2012:17

Adaptive FEM with relaxation for a hyperbolic coefficient inverse problem

LARISA BEILINA
MICHAEL V. KLIBANOV

Department of Mathematical Sciences
Division of Mathematics
CHALMERS UNIVERSITY OF TECHNOLOGY
UNIVERSITY OF GOTHENBURG
Gothenburg Sweden 2012

Preprint 2012:17

Adaptive FEM with relaxation for a hyperbolic coefficient inverse problem

Larisa Beilina and Michael V. Klibanov

Department of Mathematical Sciences
Division of Mathematics
Chalmers University of Technology and University of Gothenburg
SE-412 96 Gothenburg, Sweden
Gothenburg, September 2012

Preprint 2012:17
ISSN 1652-9715

Matematiska vetenskaper
Göteborg 2012

Adaptive FEM with relaxation for a hyperbolic coefficient inverse problem

Larisa Beilina * and Michael V. Klibanov †

Recent research of publications [6, 7, 9, 10, 11, 12, 13, 14, 15, 17] have shown that adaptive finite element method presents a useful tool for solution of hyperbolic coefficient inverse problems. In the above publications improvement in the image reconstruction is achieved by local mesh refinements using a posteriori error estimate in the Tikhonov functional and in the reconstructed coefficient. In this paper we apply results of the above publications and present the relaxation property for the mesh refinements and a posteriori error estimate for the reconstructed coefficient for a hyperbolic CIP, formulate an adaptive algorithm and apply it to the reconstruction of the coefficient in hyperbolic PDE. Our numerical examples presents performance of the two-step numerical procedure on the computationally simulated data where on the first step we obtain good approximation of the exact coefficient using approximate globally convergent method of [12], and on the second step we take this solution for further improvement via adaptive mesh refinements.

1 Introduction

In this paper we summarize recent results on the Adaptive Finite Element Method (adaptivity) for solution of hyperbolic coefficient inverse problem, see [1, 6, 7, 9, 10, 11, 13, 14, 15, 17] and chapter 4 of [12]. We also present relaxation property in adaptivity which is based on results of [17] and reformulate theorems of [17] for our specific case of hyperbolic CIP.

The relaxation property means that the accuracy of the computed solution improves with mesh refinements of the initial mesh. The relaxation property in the

* Department of Mathematical Sciences, Chalmers University of Technology and Gothenburg University, SE-42196 Gothenburg, Sweden, (larisa@chalmers.se)

† Department of Mathematics and Statistics University of North Carolina at Charlotte, Charlotte, NC 28223, USA, (mklibanv@uncc.edu)

adaptive finite element method applied to the solution of CIPs was observed numerically in many publications, see, e.g. [1, 6, 7, 9, 10, 11, 13, 14, 15]. Analytically it was proved for the first time in [17].

The adaptivity for acoustic and elastic CIPs was developed by the first author in her PhD thesis in 2003 [8] with the first publication [6]. A similar idea was proposed in [4]. However, an example of a CIP was not considered in [4]. The adaptivity was developed further in a number of publications, where it was applied both to CIPs [3, 6, 7, 9, 10, 11] and to the parameter identification problems, which are different from CIPs to some other ill-posed problems, see, e.g. [22, 24, 25]. In [35] the adaptivity was applied to the Cauchy problem for the Laplace equation. In the recent publication [32] was developed an adaptive finite element method for the solution of the Fredholm integral equation of the first kind.

The idea of adaptivity consists in the minimization of the Tikhonov functional on a sequence of locally refined meshes using a posteriori error estimates. We note that due to local mesh refinements, the total number of finite elements is rather moderate and the corresponding finite element space behaves as a finite dimensional one. Since all norms in finite dimensional spaces are equivalent, then we use the same norm in the Tikhonov regularization term as the one in the original space. This is obviously more convenient for both analysis and numerical studies of this and previous publications than the standard case of a stronger norm [2, 12, 26, 38, 39] in this term. Numerical results of the current and previous publications [6, 7, 9, 10, 11] confirm the validity of this approach.

In section 3 of this paper we present a posteriori error estimates of distances between regularized solutions and ones obtained after mesh refinements. In the past publications which uses the adaptivity for ill-posed problems such estimates were obtained only for some functionals rather than for solutions themselves, see, e.g. [4, 6, 7, 10, 11, 13, 14, 24, 25].

Because of the well known phenomenon of local minima and ravines of the Tikhonov functional, many regularized solutions might exist. Furthermore, even if such a regularized solution exists and is unique, it is unclear how to practically find it, unless a good first guess about the true solution is available. Recently developed the approximately globally convergent method for CIPs for a hyperbolic PDE with single measurement data, see, e.g. [12, 13, 14, 15, 17, 31, 17, 33] and further referenced cited there delivers a such good approximation for the exact solution.

In our numerical examples we use the two-step numerical procedure which was developed for some CIPs for a hyperbolic PDE [12, 13, 14, 15]. On the first step, the approximately globally convergent method delivers a good approximation for the exact solution, and on the second step, the adaptivity uses this approximation as a starting point for a refinement. We need the first step since the adaptivity works only in a small neighborhood of the exact solution of the Tikhonov functional. Numerical examples of section 6 presents results of the reconstruction of the unknown coefficient of hyperbolic PDE using this two-step numerical procedure.

2 The Space of Finite Elements

First we introduce the space of standard piecewise linear finite elements, which are triangles in 2-d and tetrahedra in 3-d. Let $\Omega \subset \mathbb{R}^n, n = 2,3$ be a bounded domain. Let a triangulation T of Ω represents a coarse mesh. Following section 76.4 of [21], we construct global piecewise linear functions $\left\{e_j(x,T)\right\}_{j=1}^{p(T)} \subset C\left(\overline{\Omega}\right)$ associated with the triangulation T. Functions $\left\{e_j(x,T)\right\}_{j=1}^{p(T)}$ are linearly independent in Ω and its number equals to the number of the mesh points in the domain Ω.

Let $\{N_i\} = N_1, N_2, ..., N_{p(T)}$ be the enumeration for nodes in the triangulation T. Then test functions satisfies to the condition for all $i, j \in \{N_i\}$

$$e_j(N_i,T) = \begin{cases} 1, i = j, \\ 0, i \neq j. \end{cases}$$

Let $V_h(T)$ is the linear space of finite elements with its basis $\left\{e_j(x,T)\right\}_{j=1}^{p(T)}$ which is defined as

$$V_h(T) = \{v(x) \in V : v\,|_K \in P_1(K)\ \forall K \in T\}, \tag{1}$$

where $P_1(K)$ defines the set of linear functions on K and

$$V(T) = \left\{v(x) : v \in C\left(\overline{\Omega}\right), \nabla v \in P(C(\Omega))\right\}.$$

Here, $P(C(\Omega))$ defines the set of piecewise-continuous functions on Ω. In (1) $v\,|_K$ is the function defined on the element K which coincides with v on K. Each function $v \in V_h(T)$ can be represented as

$$v(x) = \sum_{j=1}^{p(T)} v(N_j) e_j(x,T).$$

Let $h(K_j)$ be the diameter of the triangle/tetrahedra $K_j \subset T$. We define the mesh parameter h

$$h = \max_{K_j \subset T} h(K_j) \tag{2}$$

and call it by the *maximal grid step size* of the triangulation T. Let r be the radius of the maximal circle/sphere inscribed in K_j. We impose the following shape regularity assumption for all triangles/tetrahedra uniformly for all possible triangulations T

$$a_1 \leqslant h(K_j) \leqslant r a_2, \quad a_1, a_2 = const. > 0,\ \forall K_j \subset T,\ \forall\, T, \tag{3}$$

where numbers a_1, a_2 are independent on the triangulation T. We also assume that the following condition is fulfilled

$$h(K_j)/h(K_i) \leq C \tag{4}$$

with the some constant C, where $h(K_j), h(K_i)$ are the smallest and the largest diameters for the elements in the mesh T_n, correspondingly. Condition (4) practically means that we can not refine the mesh infinitely and we should check both conditions (2) and (4) simultaneously after every mesh refinement.

Usually, the number of all triangulations which are satisfying (3) is finite, and we define the following finite dimensional linear space H,

$$H = \bigcup_T Span(V_h(T)),\ \forall T \ \text{ satisfying (3).}$$

Hence,

$$\dim H < \infty,\ H \subset \left(C\left(\overline{\Omega}\right) \cap H^1(\Omega)\right),\ \partial_{x_i} f \in L_\infty(\Omega),\ \forall f \in H. \tag{5}$$

In (5) "$\subset$" means the inclusion of sets. We equip H with the same inner product as the one in $L_2(\Omega)$. Denote $(,)$ and $\|\cdot\|$ the inner product and the norm in H respectively, $\|f\|_H := \|f\|_{L_2(\Omega)} := \|f\|, \forall f \in H$. We refer to [12, 17] for description of the construction of subspaces of triangulations $\{T_n\}$ as well as corresponding subspaces $\{M_n\}$ of the space H. We view the space H as an "ideal" space of very fine finite elements. This space cannot be reached in practical computations.

Let I be the identity operator on H. For any subspace $M \subset H$, let $P_M : H \to M$ be the orthogonal projection operator onto M. Denote $P_n := P_{M_n}$. Let h_n be the mesh function for T_n defined as a maximal diameter of the elements in triangulation T_n. Let f_n^I be the standard interpolant of the function $f \in H$ on triangles/tetrahedra of T_n, see section 76.4 of [21]. It can be easily derived from formula (76.3) of [21] that

$$\left\| f - f_n^I \right\|_{L_\infty(\Omega)} \leq K \|\nabla f\|_{L_\infty(\Omega)} h_n, \forall f \in H, \tag{6}$$

where $K = K(\Omega, r, a_1, a_2) = const. > 0$. Since $f_n^I \in H, \forall f \in H$, then by one of well known properties of orthogonal projection operators,

$$\|f - P_n f\| \leqslant \left\| f - f_n^I \right\|,\ \forall f \in H. \tag{7}$$

Hence, from (6) and (7) follows that

$$\|f - P_n f\|_{L_\infty(\Omega)} \leqslant K \|\nabla f\|_{L_\infty(\Omega)} h_n, \forall f \in H. \tag{8}$$

Since H is a finite dimensional space in which all norms are equivalent, it is convenient for us to rewrite (8) with a different constant K in the form

$$\|x - P_n x\| \leqslant K \|x\| h_n,\ \forall x \in H. \tag{9}$$

3 Relaxation property for a Coefficient Inverse Problem

In section below we present theorems which show the relaxation property for hyperbolic CIP. More explicitly, we prove that the accuracy of the solution of hyperbolic CIP improves with mesh refinements. Proofs of these theorems follows from the results of section 4 of [12].

3.1 Coefficient Inverse Problem and Tikhonov functional

We consider a convex bounded domain $\Omega \subset \mathbb{R}^3$ with the boundary $\partial\Omega \in C^3$. Let the point $x_0 \notin \overline{\Omega}$.

Denote $Q_T = \Omega \times (0,T), S_T = \partial\Omega \times (0,T)$ for $T > 0$. Let $d > 1$ be a number, $\omega \in (0,1)$ be a sufficiently small number, and the function $c(x) \in C\left(\mathbb{R}^3\right)$ belongs to the set of admissible coefficients M_c such that

$$M_c = \{c(x) : c(x) \in (1-\omega, d+\omega) \text{ in } \Omega, c(x) = 1 \text{ outside of } \Omega\}. \tag{10}$$

In numerical experiments we specify $c(x) > 1$. Consider the solution $u(x,t)$ of the following Cauchy problem

$$c(x)\, u_{tt} = \Delta u, x \in \mathbb{R}^3, t \in (0,T), \tag{11}$$

$$u(x,0) = 0, u_t(x,0) = \delta(x - x_0). \tag{12}$$

Equation (11) is called the acoustic wave equation in the case x is the sound speed and $u(x,t)$ is the amplitude of the acoustic wave [40]. Equation (11) also governs propagation of the electromagnetic field with $c(x) = \varepsilon_r(x)$, where $\varepsilon_r(x)$ is the spatially distributed dielectric constant. [37].

In (12) the point source can be replaced with the incident plane wave in the case when it is initialized at the plane $\{x_3 = x_{3,0}\}$ such that $\{x_3 = x_{3,0}\} \cap \overline{\Omega} = \varnothing$. All derivations below are similar to the case of plane wave too. In our Theorems below we focus on (12), but in numerical studies we use the incident plane wave.

Coefficient Inverse Problem (CIP**)**. Let conditions (10)-(12) hold. Assume that the coefficient $c(x)$ is unknown inside the domain Ω. Determine this coefficient for $x \in \Omega$, assuming that the following function $g(x,t)$ is known

$$u|_{S_T} = g(x,t). \tag{13}$$

The function $g(x,t)$ represents measurements of the outcome wave field $u(x,t)$ at the boundary of the domain of interest Ω. Since the function $c(x) = 1$ outside of Ω, then (11)-(13) imply

$$u_{tt} = \Delta u, (x,t) \in \left(\mathbb{R}^3 \setminus \Omega\right) \times (0,T),$$

$$u(x,0) = u_t(x,0) = 0, x \in \mathbb{R}^3 \setminus \Omega, u|_{S_T} = g(x,t).$$

Solving this initial boundary value problem for $(x,t) \in \left(\mathbb{R}^3 \setminus \Omega\right) \times (0,T)$, we uniquely obtain Neumann boundary condition $p(x,t)$ for the function u,

$$\partial_n u \mid_{S_T} = p(x,t). \tag{14}$$

Since CIPs are complex problems one naturally needs to impose some simplifying assumptions. In the case of our particular CIP uniqueness theorem for our CIP does not working unless we replace the $\delta-$function in (12) by a smooth function, which approximates $\delta(x-x_0)$ in the distribution sense. Let $\varkappa \in (0,1)$ be a sufficiently small number. We replace $\delta(x-x_0)$ in (12) with the function $\delta_\varkappa(x-x_0)$,

$$\delta_\varkappa(x-x_0) = \begin{cases} C_\varkappa \exp\left(\frac{1}{|x-x_0|^2-\varkappa^2}\right), |x-x_0| < \varkappa, \\ 0, |x-x_0| > \varkappa, \end{cases} \int\limits_{\mathbb{R}^3} \delta_\varkappa(x-x_0)\,dx = 1. \tag{15}$$

We assume that $\varkappa$ is so small that

$$\delta_\varkappa(x-x_0) = 0 \text{ in } \overline{\Omega}. \tag{16}$$

Let $\zeta \in (0,1)$ be a sufficiently small number. Consider the function $z_\zeta \in C^\infty[0,T]$ such that

$$z_\zeta(t) = \begin{cases} 1, t \in [0, T-2\zeta], \\ 0, t \in [T-\zeta, T], \\ \text{between 0 and 1 for } t \in [0, T-2\zeta, T-\zeta]. \end{cases} \tag{17}$$

Let us consider the following state problem

State Problem. Find the solution $v(x,t)$ of the following initial boundary value problem

$$\begin{aligned} c(x)\,v_{tt} - \Delta v = 0 \text{ in } Q_T, \\ v(x,0) = v_t(x,0) = 0, \\ \partial_n v \mid_{S_T} = p(x,t). \end{aligned} \tag{18}$$

The Tikhonov functional for the above CIP which corresponds to the state problem (18) is

$$E_\alpha(c) = \frac{1}{2}\int\limits_{S_T} (v \mid_{S_T} - g(x,t))^2 z_\zeta(t)\,d\sigma dt + \frac{1}{2}\alpha \int\limits_{\Omega} (c - c_{glob})^2 dx, \tag{19}$$

where c_{glob} is the approximate solution obtained by an approximately globally convergent numerical method of [12] on the first stage of our two stage numerical procedure (introduction and [12, 13]) and α is the small regularization parameter. To figure out the Fréchet derivative of the functional $E_\alpha(c)$, we introduce the Lagrangian $L(\lambda, v, c)$,

$$L(\lambda, v, c) = E_\alpha(c) - \int\limits_{Q_T} c(x) v_t \lambda_t dx dt + \int\limits_{Q_T} \nabla v \nabla \lambda\, dx dt - \int\limits_{S_T} p\lambda\, d\sigma_x dt. \tag{20}$$

The sum of integral terms in $L(c)$ equals zero, because of the definition of the weak solution $v \in H^1$ of the problem (18) as $v(x,0) = 0$ and

$$\int\limits_{Q_T} (-c(x) v_t w_t + \nabla v \nabla w)\, dxdt - \int\limits_{S_T} pwd\sigma_x dt = 0, \forall w \in H^1(Q_T), w(x,T) = 0, \quad (21)$$

see section 5 of Chapter 4 of [34]. Hence, $L(c) = E_\alpha(c)$. To find the Fréchet derivative of the Lagrangian (20) it is necessary to consider Fréchet derivatives of functions v, λ with respect to the coefficient c (in certain functional spaces). This in turn requires to establish a higher smoothness of functions v, λ than just $H^1(Q_T)$ [12, 14].

The Fréchet derivative of the Lagrangian with respect to λ gives us the state problem and the Fréchet derivative of the Lagrangian with respect to v gives us the adjoint problem which we present below.

Adjoint Problem. Find the solution $\lambda(x,t)$ of the following initial boundary value problem with the reversed time

$$\begin{aligned} c(x)\lambda_{tt} - \Delta\lambda &= 0 \text{ in } Q_T, \\ \lambda(x,T) &= \lambda_t(x,T) = 0, \\ \partial_n \lambda\,|_{S_T} &= z_\zeta(t)(g-v)(x,t). \end{aligned} \quad (22)$$

In (18) and (22) functions $v \in H^1(Q_T)$ and $\lambda \in H^1(Q_T)$ are weak solutions of problems (18) and (22) respectively. In fact, we need a higher smoothness of these functions, which we specify below. In (22) and (18) functions g and p are the ones from (13) and (14) respectively. Hence, to solve the adjoint problem, one should solve the state problem first. The function $z_\zeta(t)$ is introduced to ensure the validity of compatibility conditions at $\{t = T\}$ in (22).

State and adjoint problems are concerned only with the domain Ω rather than with the entire space $\mathbb{R}^3$. We define the space Z as

$$Z = \left\{ f : f \in C\left(\overline{\Omega}\right) \cap H^1(\Omega), c_{x_i} \in L_\infty(\Omega), i = 1,2,3 \right\}, \|f\|_Z = \|f\|_{C\left(\overline{\Omega}\right)} + \sum_{i=1}^{3} \|f_{x_i}\|_{L_\infty(\Omega)}.$$

Clearly $H \subset Z$ as a set. To apply the theory of above sections, we express in subsection 6.2 the function $c(x)$ via standard piecewise linear finite elements. Hence, we assume below that $c \in Y$, where

$$Y = \{c \in Z : c \in (1-\omega, d+\omega)\}. \quad (23)$$

Theorem 3.1.1 can be easily derived from a combination of Theorems 4.7.1, 4.7.2 and 4.8 of [12] as well as from Theorems 3.1, 3.2 of [14].

Theorem 3.1.1. *Let $\Omega \subset \mathbb{R}^3$ be a convex bounded domain with the boundary $\partial\Omega \in C^2$ and such that there exists a function $a \in C^2\left(\overline{\Omega}\right)$ such that $a\,|_{\partial\Omega} = 0, \partial_n a\,|_{\partial\Omega} = 1$. Assume that there exists functions $P(x,t), \Phi(x,t)$ such that*

$$P \in H^6(Q_T), \Phi \in H^5(Q_T); \partial_n P|_{S_T} = p(x,t), \partial_n \Phi|_{S_T} = z_\zeta(t) g(x,t),$$
$$\partial_t^j P(x,0) = \partial_t^j \Phi(x,0) = 0, j = 1,2,3,4.$$

Then for every function $c \in Y$ functions $v, \lambda \in H^2(Q_T)$, where v, λ are solutions of state and adjoint problems (18), (22). Also, for every $c \in Y$ there exists Fréchet derivative $E'_\alpha(c)$ of the Tikhonov functional $E_\alpha(c)$ in (19) and

$$E'_\alpha(c)(x) = \alpha\left(c - c_{glob}\right)(x) - \int_0^T (u_t \lambda_t)(x,t)\, dt := \alpha\left(c - c_{glob}\right)(x) + y(x). \quad (24)$$

The function $y(x) \in C\left(\overline{\Omega}\right)$ and the there exists a constant $B = B\left(\Omega, a, d, \omega, z_\zeta\right) > 0$ such that

$$\|y\|_{C(\overline{\Omega})} \leq \|c\|^2_{C(\overline{\Omega})} \exp(BT) \left(\|P\|^2_{H^6(Q_T)} + \|\Phi\|^2_{H^5(Q_T)}\right). \quad (25)$$

The functional of the Fréchet derivative $E'_\alpha(c)$ acts on any function $b \in Z$ as

$$E'_\alpha(c)(b) = \int_\Omega E'_\alpha(c)(x) b(x)\, dx.$$

3.2 Relaxation property for the functional $E_\alpha(c)$

We now specify the relaxation property of [17] for the specific functional $E_\alpha(c)$ for our CIP. Let Y be the set of functions defined in (23) and H be the finite dimensional space of finite elements constructed in section 2. We define the set G as $G := Y \cap H$. We consider the set G as the subset of the space H with the same norm as in H. In particular, $\overline{G} = \left\{c(x) \in H : c(x) \in [1-\omega, d+\omega] \text{ for } x \in \overline{\Omega}\right\}$. Let the Hilbert space $H_2 := L_2(S_T)$. We define the operator F as

$$F : \overline{G} \to H_2, F(c)(x,t) = z_\zeta(t)\left[g(x,t) - v(x,t,c)\right], \ (x,t) \in S_T, \quad (26)$$

where the function $v := v(x,t,c)$ is the weak solution (21) of the state problem (18), g is the function in (13) and $z_\zeta(t)$ is the function defined in (17). For any function $b \in H$ consider the weak solution $\widetilde{u}(x,t,c,b) \in H^1(Q_T)$ of the following initial boundary value problem

$$c(x)\widetilde{u}_{tt} = \Delta\widetilde{u} - b(x) v_{tt}, (x,t) \in Q_T,$$
$$\widetilde{u}(x,0) = \widetilde{u}_t(x,0) = 0, \widetilde{u}|_{S_T} = 0.$$

Theorem 3.2.2 can be easily derived from a combination of Theorems 4.7.2 and 4.10 of [12].

Theorem 3.2.2. *Let $\Omega \subset \mathbb{R}^3$ be a convex bounded domain with the boundary $\partial\Omega \in C^2$. Suppose that there exist functions $a(x), P(x,t), \Phi(x,t)$ satisfying conditions of Theorem 3.1.1. Then the function $\widetilde{u}(x,t,c,b) \in H^2(Q_T)$. Also, the operator F in (26) has the Fréchet derivative $F'(c)(b)$,*

$$F'(c)(b) = -z_\zeta(t)\,\widetilde{u}(x,t,c,b)\,|_{S_T}, \forall c \in G, \forall b \in H.$$

Let $B = B\left(\Omega, a, d, \omega, z_\zeta\right) > 0$ be the constant of Theorem 3.1.1. Then

$$\left\|F'(c)\right\|_{\mathscr{L}} \leq \exp(CT)\,\|P\|_{H^6(Q_T)},\ \forall c \in G.$$

In addition, the operator $F'(c)$ is Lipschitz continuous,

$$\left\|F'(c_1) - F'(c_2)\right\|_{\mathscr{L}} \leq \exp(CT)\,\|P\|_{H^6(Q_T)}\,\|c_1 - c_2\|,\ \forall c_1, c_2 \in G.$$

We also introduce the error of the level δ in the data $g(x,t)$ in (13). So, we assume that

$$g(x,t) = g^*(x,t) + g_\delta(x,t);\ g^*, g_\delta \in L_2(S_T), \|g_\delta\|_{L_2(S_T)} \leq \delta. \tag{27}$$

where $g^*(x,t)$ is the exact data and the function $g_\delta(x,t)$ represents the error in these data. To make sure that the operator F is one-to-one, we need to refer to a uniqueness theorem for our CIP. However, uniqueness results for multidimensional CIPs with single measurement data are currently known only under the assumption that at least one of initial conditions does not equal zero in the entire domain $\overline{\Omega}$, which is not our case.

All these uniqueness theorems were proven by the method of Carleman estimates, which was originated in 1981 simultaneously and independently by the authors of the papers [18, 19, 27]; also see, e.g. [20, 28, 29, 30] as well as sections 1.10, 1.11 of the book [12] and references cited there. However, because of applications, it makes sense to develop numerical methods for the above CIP, regardless on the absence of proper uniqueness theorems. Therefore, we introduce Assumption 3.2.1.

Assumption 3.2.1. *The operator $F(c)$ defined in (26) is one-to-one.*

Theorem 3.2.3 follows from Theorems 3.3 of [16], 3.1.1 and 3.2.2. Note that if a function $c \in H$ is such that $c \in [1,d]$, then $c \in G$.

Theorem 3.2.3. *Let $\Omega \subset \mathbb{R}^3$ be a convex bounded domain with the boundary $\partial\Omega \in C^3$. Suppose that there exist functions $a(x), P(x,t), \Phi(x,t)$ satisfying conditions of Theorem 3.1.1. Let Assumption 3.2.1 and condition (27) hold. Let the function $v = v(x,t,c) \in H^2(Q_T)$ in (19) be the solution of the state problem (18) for the function $c \in G$. Assume that there exists the exact solution $c^* \in G, c^*(x) \in [1,d]$ of the equation $F(c^*) = 0$ for the case when in (27) the function g is replaced with the function g^*. Let in (27)*

$$\alpha = \alpha(\delta) = \delta^{2\mu}, \mu = const. \in (0, 1/4).$$

Also, let in (19) the function $c_{glob} \in G$ be such that

$$\left\|c_{glob} - c^*\right\| < \frac{\delta^{3\mu}}{3}.$$

Then there exists a sufficiently small number $\delta_0 = \delta_0\left(\Omega, d, \omega, z_\zeta, a, \|P\|_{H^6(Q_T)}, \mu\right) \in (0,1)$ such that for all $\delta \in (0,\delta_0)$ the neighborhood $V_{\delta^{3\mu}}(c^*)$ of the function c^* is such that $V_{\delta^{3\mu}}(c^*) \subset G$ and the functional $E_\alpha(c)$ is strongly convex in $V_{\delta^{3\mu}}(c^*)$ with the strong convexity constant $\alpha/4$. In other words,

$$\|c_1 - c_2\|^2 \leq \frac{2}{\delta^{2\mu}}\left(E'_\alpha(c_1) - E'_\alpha(c_2), c_1 - c_2\right), \ \forall c_1, c_2 \in G, \tag{28}$$

where $(,)$ is the scalar product in $L_2(\Omega)$ and the Fréchet derivative E'_α is calculated as in (24). Furthermore, there exists the unique regularized solution $c_{\alpha(\delta)}$, and $c_{\alpha(\delta)} \in V_{\delta^{3\mu}/3}(x^*)$. In addition, the gradient method of the minimization of the functional $E_\alpha(c)$, which starts at c_{glob}, converges to $c_{\alpha(\delta)}$. Furthermore, let $\xi \in (0,1)$ be an arbitrary number. Then there exists a number $\delta_1 = \delta_1\left(\Omega, d, \omega, z_\zeta, a, \|P\|_{H^6(Q_T)}, \mu, \xi\right) \in (0,\delta_0)$ such that

$$\left\|c_{\alpha(\delta)} - c^*\right\| \leq \xi \left\|c_{glob} - c^*\right\|, \ \forall \delta \in (0,\delta_1).$$

In other words, the regularized solution $c_{\alpha(\delta)}$ provides a better accuracy than the solution obtained on the first stage of our two-stage numerical procedure. Furthermore, (28) implies that

$$\left\|c - c_{\alpha(\delta)}\right\| \leq \frac{2}{\delta^{2\mu}}\left\|E'_\alpha(c)\right\|_{L_2(\Omega)}. \tag{29}$$

Theorem 3.2.4 is follows from Theorems 5.1 of [16] and 3.2.3 as well as from Theorem 4.11.3 of [12].

Theorem 3.2.4. *Let conditions of Theorem 3.2.3 hold. Let $\|c^*\| \leq A$, where the constant A is given. Let $M_n \subset H$ be the subspace obtained after n mesh refinements as described in section 2. Let h_n be the maximal grid step size of the subspace M_n. Let $B = B\left(\Omega, a, d, \omega, z_\zeta\right) > 0$ be the constant of Theorem 3.1.1 and K be the constant in (9). Then there exists a constant $\overline{N}_2 = \overline{N}_2\left(\exp(CT)\|P\|_{H^6(Q_T)}\right)$ such that if*

$$h_n \leq \frac{\delta^{4\mu}}{A\overline{N}_2 K},$$

then there exists the unique minimizer c_n of the functional (19) on the set $G \cap M_n$, $c_n \in V_{\delta^{3\mu}}(x^*) \cap M_n$ and the following a posteriori error estimate holds

$$\left\|c_n - c_{\alpha(\delta)}\right\| \leq \frac{2}{\delta^{2\mu}}\left\|E'_{\alpha(\delta)}(c_n)\right\|_{L_2(\Omega)}. \tag{30}$$

The estimate (30) is *a posteriori* because it is obtained after the function c_n is calculated. Theorem 3.2.5 follows from Theorems 5.2, 5.3, 3.2.4 as well as from Theorem 4.11.4 of [12].

Theorem 3.2.5 (relaxation property of the adaptivity)**.** *Assume that conditions of Theorem 3.2.4 hold. Let $c_n \in V_{\delta^{3\mu}}(x^*) \cap M_n$ be the unique minimizer of the Tikhonov functional (19) on the set $G \cap M_n$ (Theorem 3.2.4). Assume that the regularized solution $c_{\alpha(\delta)} \neq c_n$, i.e. $c_{\alpha(\delta)} \notin M_n$. Let $\eta \in (0,1)$ be an arbitrary number. Then one can choose the maximal grid size $h_{n+1} = h_{n+1}\left(A, \overline{N}_2, K, \delta, z_\zeta, \mu, \eta\right) \in (0, h_n]$ of the mesh refinement number $(n+1)$ so small that*

$$\left\|c_{n+1} - c_{\alpha(\delta)}\right\| \leq \eta \left\|c_n - c_{\alpha(\delta)}\right\| \leq \frac{2\eta}{\delta^{2\mu}} \left\|E'_{\alpha(\delta)}(c_n)\right\|_{L_2(\Omega)}, \tag{31}$$

where the number $\overline{N}_2$ was defined in Theorem 3.2.4. Let $\xi \in (0,1)$ be an arbitrary number. Then there exists a sufficiently small number $\delta_0 = \delta_0\left(A, \overline{N}_2, K, \delta, z_\zeta, \xi, \mu, \eta\right) \in (0,1)$ and a decreasing sequence of maximal grid step sizes $\{h_k\}_{k=1}^{n+1}$, $h_k = h_k\left(A, \overline{N}_2, K, \delta, z_\zeta, \xi, \mu.\eta\right)$ such that if $\delta \in (0, \delta_0)$, then

$$\|c_{k+1} - c^*\| \leq \eta^k \left\|c_1 - c_{\alpha(\delta)}\right\| + \xi \left\|c_{glob} - c^*\right\|, k = 1, ..., n. \tag{32}$$

Theorem 3.2.6 follows from Theorems 5.4 of [16] and 3.2.5.

Theorem 3.2.6. (relaxation property of the adaptivity for local mesh refinements). *Assume that conditions of Theorem 3.2.5 hold. Let $\Omega = \Omega_1 \cup \Omega_2$. Suppose that mesh refinements are performed only in the subdomain Ω_2. Let $h^{(1)}$ be the maximal grid step size in Ω_1. Then there exists a sufficiently small number $\delta_0 = \delta_0\left(A, \overline{N}_2, K, \delta, z_\zeta, \xi, \mu, \eta\right) \in (0,1)$ and a decreasing sequence of maximal grid step sizes $\left\{\widetilde{h}_k\right\}_{k=1}^{n+1}$, $\widetilde{h}_k = \widetilde{h}_k\left(A, \overline{N}_2, K, \delta, z_\zeta, \xi, \mu, \eta\right)$ of meshes in Ω_2 such that if $\left\|\nabla c_{\alpha(\delta)}\right\|_{L_\infty(\Omega_1)}$ is so small that if*

$$\frac{2K\overline{N}_3}{\delta^{2\mu}} \left\|\nabla c_{\alpha(\delta)}\right\|_{L_\infty(\Omega_1)} h^{(1)} \leq \frac{\eta}{2} \left\|c_k - c_{\alpha(\delta)}\right\|, k = 1, ..., n \text{ and } \delta \in (0, \delta_0),$$

then (32) holds with the replacement of $\{h_k\}_{k=1}^{n+1}$ with $\left\{\widetilde{h}_k\right\}_{k=1}^{n+1}$. Here the number $\overline{N}_3$ depends on the same parameters as $\overline{N}_2$.

4 Mesh Refinement Recommendations

We now present recommendations for mesh refinements which are based on the theory of section 3.

The First Mesh Refinement Recommendation. *Refine the mesh in neighborhoods of those grid points $x \in \Omega_2$ where the function $|E'_\alpha(c_n)(x)|$ attains its maximal values, where the function $|E'_\alpha(c_n)(x)|$ is given by formula (24). More precisely, let*

$\beta_1 \in (0,1)$ be the tolerance number. Refine the mesh in such subdomains of Ω_2 where

$$\left|E'_\alpha(c_n)(x)\right| \geq \beta_1 \max_{\overline{\Omega}_2} \left|E'_\alpha(c_n)(x)\right|. \tag{33}$$

To figure out the second mesh refinement recommendation, we note that by (24) and (25)

$$\left|E'_{\alpha(\delta)}(c_n)(x)\right| \leq \alpha\left(\|c_n\|_{C(\overline{\Omega})} + \left\|c_{glob}\right\|_{C(\overline{\Omega})}\right) + \|c_n\|^2_{C(\overline{\Omega})} \exp(CT)\left(\|P\|^2_{H^6(Q_T)} + \|\Phi\|^2_{H^5(Q_T)}\right).$$

Since α is small, then the second term in the right hand side of this estimate dominates. Next, since we have decided to refine the mesh in neighborhoods of those points, which deliver maximal values for the function $\left|E'_{\alpha(\delta)}(c_n)(x)\right|$, then we obtain the following mesh refinement recommendation.

Second Mesh Refinement Recommendation. *Refine the mesh in neighborhoods of those grid points $x \in \Omega_2$ where the function $c_n(x)$ attains its maximal values. More precisely, let $\beta_2 \in (0,1)$ be the tolerance number. Refine the mesh in such subdomains of Ω_2 where*

$$c_n(x) \geq \beta_2 \max_{\overline{\Omega}_2} c_n(x), \tag{34}$$

How to choose numbers β_1 and β_2, depends on numerical experiments. If we would choose $\beta_1, \beta_2 \approx 1$, then we would refine the mesh in too narrow regions, and if we would choose $\beta_1, \beta_2 \approx 0$, then we would refine the mesh in almost the entire subdomain Ω_2, which is inefficient.

5 The adaptive algorithm

In this section we present our adaptive algorithm which uses the mesh refinement recommendations of section 4.

Recall that in our computations we use two-step procedure when on the first step we apply the approximately globally convergent algorithm (shortly globally convergent algorithm) of [12] and on the second step the adaptive finite element method improves this solution. In Theorem 2.9.4 of [12] was proven that the globally convergent algorithm gives solution c_{glob} which is a good approximation for the exact solution $c^*(x)$ of the above CIP. We take this first good approximation c_{glob} as an initial guess in our second step - in an adaptive algorithm.

On every mesh we find an approximate solution of the equation $E'_\alpha(c) = 0$. Hence, on every mesh we should find an approximate solution of the following equation

$$\alpha\left(c - c_{glob}\right)(x) - \int_0^T (u_t \lambda_t)(x,t)\ dt = 0.$$

For each newly refined mesh we first linearly interpolate the function $c_{glob}(x)$ on it and iteratively update approximations c_h^m of the function c_h, where m is the number of iteration in optimization procedure. To do so, we use the quasi-Newton method with the classic BFGS update formula with the limited storage [36]. Denote

$$g^m(x) = \alpha(c_h^m - c_{glob})(x) - \int_0^T (u_{ht}\lambda_{ht})(x,t,c_h^m)\,dt,$$

where functions $u_h\left(x,t,c_h^m\right), \lambda_h\left(x,t,c_h^m\right)$ are computed finite element solutions of state and adjoint problems with $c := c_h^m$.

Using the mesh refinement recommendations of section 4, we apply the following adaptivity algorithm in our computations:

Adaptive algorithm

- Step 0. Choose an initial mesh K_h in Ω and an initial time partition J_0 of the time interval $(0,T)$. Start with the initial approximation $c_h^0 := c_{glob}$ and compute the sequence of c_h^m via the following steps:
- Step 1. Compute solutions $u_h = u_h\left(x,t,c_h^m\right)$ and $\lambda_h = \lambda_h\left(x,t,c_h^m\right)$ of state (18) and adjoint (22) problems, respectively, on K_h and J_k.
- Step 2. Update the coefficient $c_h := c_h^{m+1}$ on K_h and J_k using the quasi-Newton method, see details in [6, 36]

  $$c_h^{m+1} = c_h^m + \gamma H^m g^m(x),$$

  where γ is the step-size in the gradient update given by one-dimensional search algorithm [23] and H is given by the usual BFGS update formula of the Hessian [36].
- Step 3. Stop computing c_h^m and obtain the function c_h if either $||g^m||_{L_2(\Omega)} \leq \theta$ or norms $||g^m||_{L_2(\Omega)}$ are stabilized. Otherwise set $m := m+1$ and go to step 1. Here θ is the tolerance in quasi-Newton updates.
- Step 4. Compute the function $B_h(x)$,

  $$B_h(x) = \left|\alpha\,(c_h - c_{glob}) - \int_0^T \frac{\partial\lambda_h}{\partial t}\frac{\partial u_h}{\partial t}dt\right|.$$

  Next, refine the mesh at all points where

  $$B_h(x) \geq \beta_1 \max_{\overline{\Omega_2}} B_h(x). \tag{35}$$

  and where

  $$c_h(x) \geq \beta_2 \max_{\overline{\Omega_2}} c_h(x). \tag{36}$$

  Here the tolerance numbers $\beta_1, \beta_2 \in (0,1)$ are chosen by the user.
- Step 5. Construct a new mesh K_h in Ω and a new time partition J_k of the time interval $(0,T)$. On J_k the new time step τ should be chosen in such a way that the CFL condition is satisfied. Interpolate the initial approximation c_{glob} from

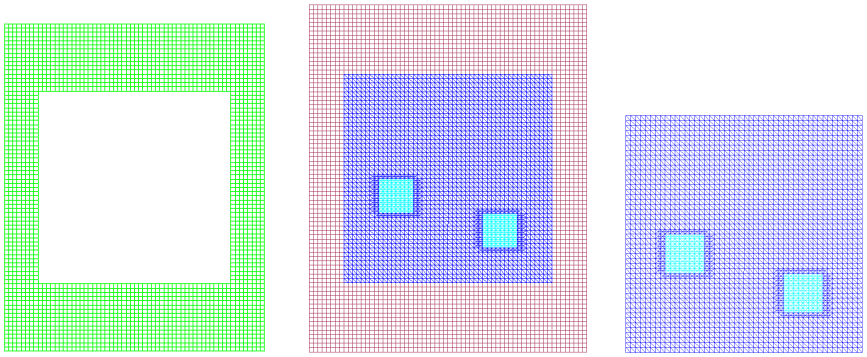

(a) G_{FDM} (b) $G = G_{FEM} \cup G_{FDM}$ (c) $G_{FEM} = \Omega$

Fig. 1 The hybrid mesh (b) is a combinations of a structured mesh (a), where FDM is applied, and a mesh (c), where we use FEM, with a thin overlapping of structured elements. The solution of the inverse problem is computed in the square Ω and $c(x) = 1$ for $x \in G \setminus \Omega$.

the previous mesh to the new mesh. Next, return to step 1 and perform all above steps on the new mesh.

- Step 6. Stop mesh refinements if norms defined in step 3 either increase or stabilize, compared with the previous mesh.

6 Numerical Studies

In this section we present performance of two-step numerical procedure on the computationally simulated data in two dimensions. In our numerical examples we work with the computationally simulated data. That is, the data are generated by computing the forward problem with the given function $c(x)$.

6.1 Computations of forward problem

To solve the forward problem, we use the hybrid FEM/FDM method described in [5] using the software package WavES [41]. The computational domain for the forward problem is $G = [-4.0, 4.0] \times [-5.0, 5.0]$. This domain is split into a finite element domain $G_{FEM} := \Omega = [-3.0, 3.0] \times [-3.0, 3.0]$ and a surrounding domain G_{FDM} with a structured mesh, $G = G_{FEM} \cup G_{FDM}$, see Figure 1. The space mesh in Ω consists of triangles and in G_{FDM} - of squares with the mesh size $\tilde{h} = 0.125$ in the overlapping regions. At the top and bottom boundaries of G we use first-order absorbing boundary conditions, and at the lateral boundaries we apply mirror boundary

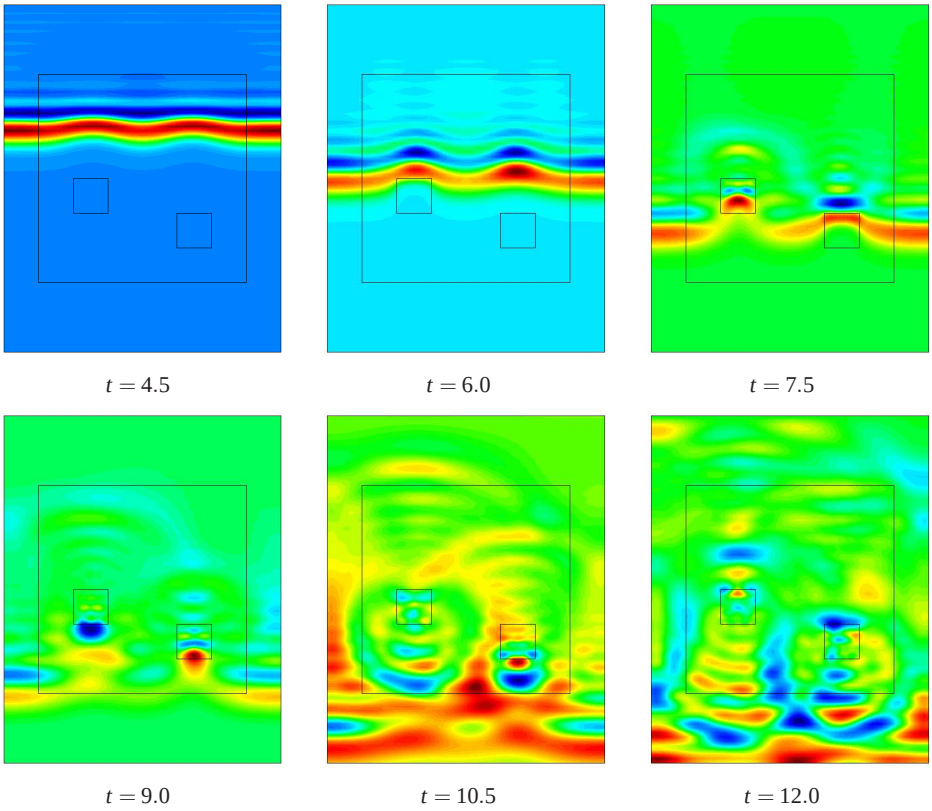

Fig. 2 Isosurfaces of the simulated exact solution to the forward problem (8.2) at different times with a plane wave initialized at the top boundary.

conditions. The coefficient $c(x)$ is unknown in the domain $\Omega \subset G$ and is defined as

$$c(x) = \begin{cases} 1 \text{ in } G \setminus \Omega \\ 1 + b(x) \text{ in } \Omega, \\ \widetilde{c} = 4 \text{ in small squares} \end{cases}, \tag{37}$$

$$b(x) = \begin{cases} A \sin^2\left(\frac{\pi x_1}{2.875}\right) \sin^2\left(\frac{\pi x_2}{2.875}\right), \text{ for } 0 < x_1 < 2.875, |x_2| < 2.875 \\ \text{and for } -2.875 < x_1 < 0, 0 < x_2 < 2.875 \\ 0 \text{ otherwise, including small squares} \end{cases}$$

Thus, (37) means that $c(x) = 1$ both near the boundary of the square Ω and outside of this square and $c(x) \geq 1 := 2d_1$ everywhere. The constant $\widetilde{c}$ characterizes the inclusion/background contrast in sharp inclusions (small squares). The number $A > 0$ is the maximal amplitude of the slowly changing background function.

The trace of the solution of the forward problem is recorded at the boundary $\partial\Omega$. Next, the coefficient $c(x)$ is "forgotten", and our goal is to reconstruct this coefficient for $x \in \Omega$ from the data $g(x,t)$. The boundary of the domain G is $\partial G = \partial G_1 \cup \partial G_2 \cup \partial G_3$. Here, ∂G_1 and ∂G_2 are respectively top and bottom sides of the largest domain of Figure 1 and ∂G_3 is the union of left and right sides of this domain. Let $t_1 := 2\pi\bar{s}^{-1}, T = 17.8t_1$. The plane wave $f(t) = 0.1(\sin(\bar{s}t - \pi/2) + 1),\ 0 \leq t \leq t_1, f(t) = 0, t \in (t_1, T)$ is initialized for $t \in (0,t_1]$ at the top boundary ∂G_1 and propagates into G. In all our tests the forward problem is

$$\begin{aligned} c(x)u_{tt} - \triangle u &= 0, \quad \text{in } G \times (0,T), \\ u(x,0) &= u_t(x,0) = 0, \text{ in } G, \\ \partial_n u\big|_{\partial G_1} &= f(t), \text{ on } \partial G_1 \times (0,t_1], \\ \partial_n u\big|_{\partial G_1} &= -\partial_t u, \text{ on } \partial G_1 \times (t_1,T), \\ \partial_n u\big|_{\partial G_2} &= -\partial_t u, \text{ on } \partial G_2 \times (0,T), \\ \partial_n u\big|_{\partial G_3} &= 0, \text{ on } \partial G_3 \times (0,T). \end{aligned} \tag{8.2}$$

6.2 Results of reconstruction using the approximately globally convergent algorithm. Test 1

In this section we present results of reconstruction using the approximately globally convergent algorithm of [12]. This algorithm gives good initial guess c_{glob} for the Tiknonov functional (19) and we take this algorithm as the first step in our two-step reconstruction procedure.

We have performed numerical experiments to reconstruct the medium shown in Figure 3-a). Here we have used value of amplitude $A = 0.5$ in (37). The plane wave f is initialized at the top boundary ∂G_1 of the computational domain G, propagates during the time period $(0,t_1]$ into G, is absorbed at the bottom boundary ∂G_2 for all times $t \in (0,T)$ and it is also absorbed at the top boundary ∂G_1 for times $t \in (t_1,T)$, see Figures 2.

To find solution c_{glob} in the approximately globally convergent algorithm we need to solve iteratively certain integral-differential equation to find functions $q_{n,i}(x,s)$ with a priori known function $V_{n,i}(x,s)$. Here s is the pseudo-frequency and indices n,i denote inner and outer iterations on every pseudo-frequency interval, respectively. For full details of implementation of this algorithm we refer to Chapter 3 of [12].

The starting value for the tail $V_{1,1}(x,\bar{s})$ was computed via solving the forward problem (8.2) for $c \equiv 1$. It was found in Chapter 3 of [12] that for domains G, Ω the pseudo-frequency interval $[\underline{s},\bar{s}] = [6.7, 7.45]$ is the optimal one. In our numerical studies we have used subinterval $[\underline{s},\bar{s}] = [6.95, 7.45]$ of the mentioned above interval. We have chosen the step size with respect to the pseudo frequency $h = 0.05$. Hence, $N = 10$ in our case. We have chosen two sequences of regularization parameters

$\lambda := \lambda_n$ and $\varepsilon = \varepsilon_n$ for $n = 1, ..., \overline{N}$,

$$\lambda_n = 20, n = 1, ..., 10;$$
$$\varepsilon_n = 0.0, n = 1, 2, \varepsilon_n = 0.0001, 2 < n \leq 10.$$

Once the function q_n is calculated, we update the function $c := c_n$, see Chapter 3 of [12] for some numerical details. The resulting computed function is $c(x) := c_{\overline{N}}(x)$. In the current work we choose stopping rule for calculation of functions q_n similar to[13]. In calculating iterations with respect to the nonlinear term (Section 5 of [13] and Chapter 3 of [12]), we consider relative norms F_n^k,

$$F_n^k = \frac{||q_{n,1}^k|_{\partial\Omega} - \overline{\psi}_n||_{L_2(\partial\Omega)}}{||\overline{\psi}_n||_{L_2}}. \tag{38}$$

with known values of $\overline{\psi}_n$. In (38) values of calculated functions $q_{n,1}^k$ are taken at the points h-inside from the lower boundary. We stop our iterations with respect to nonlinear terms when either

$$\text{either } F_n^k \geq F_n^{k-1} \text{ or } F_n^k \leq \varepsilon,$$

where $\varepsilon = 0.001$ is a small tolerance number of our choice. In other words, we stop iterations, when either F_n^k starts to grow or are too small. Next, we iterate with respect to the tails and use the same stopping criterion. Namely, we stop our iterations with respect to tails when either

$$F_{n,i} \geq F_{n,i-1} \tag{39}$$

or

$$F_{n,i} \leq \varepsilon, \tag{40}$$

where $F_{n,i} = ||q_{n,i}|_{\partial\Omega} - \overline{\psi}_n||_{L_2(\partial\Omega)}$. We denote the number of iterations with respect to tails, on which iterative procedure for function q_n is stopped, as $i := m_n$. Once the criterion (39)-(40) is satisfied, we take the last computed tail V_{n,m_n}, set $V_{n+1,1} := V_{n,m_n}$ and run computations again. Hence, the number m_n of iterations with respect to tails is chosen automatically "inside" of each iteration for q_n.

In our tests we have introduced the multiplicative random noise in the boundary data, g_σ, by adding relative error to computed data g using the following expression

$$g_\sigma\left(x^i, t^j\right) = g\left(x^i, t^j\right)\left[1 + \frac{\alpha_j(g_{max} - g_{min})\sigma}{100}\right].$$

Here, $g\left(x^i, t^j\right) = u\left(x^i, t^j\right), x^i \in \partial\Omega$ is a mesh point at the boundary $\partial\Omega, t^j \in (0, T)$ is a mesh point in time, α_j is a random number in the interval $[-1; 1]$, g_{max} and g_{min} are maximal and minimal values of the computed data g, respectively, and $\sigma = 5\%$ is the noise level.

Figure 3 displays isosurfaces of resulting images of functions $c_{n,k}, n = 2, 3, 7$ obtained in our iterative procedure. Comparison of images of functions $c_{n,k}$ for dif-

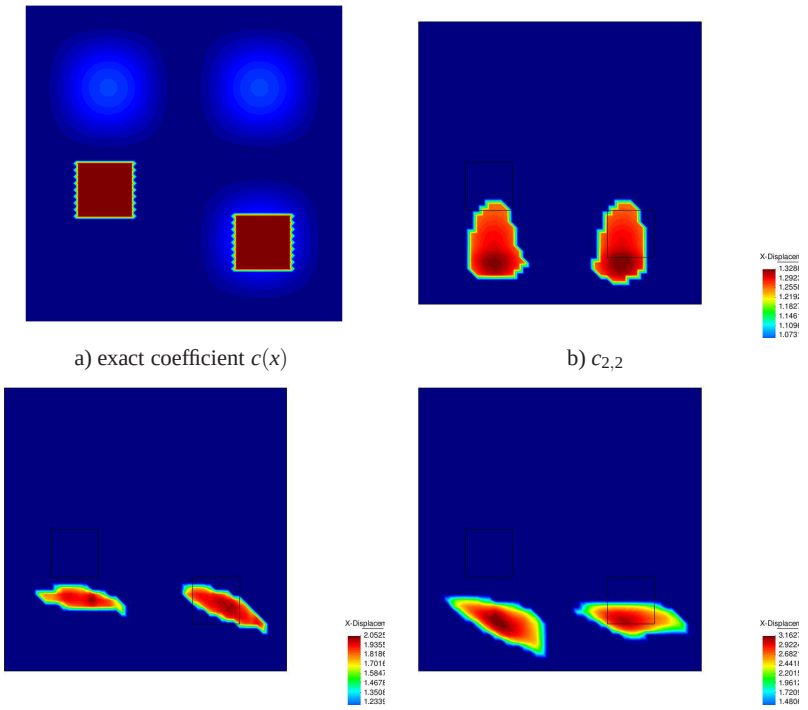

a) exact coefficient $c(x)$ b) $c_{2,2}$

c) $c_{3,12}$ d) $c_{7,9}$

Fig. 3 Test 1. Spatial distribution of exact coefficient $c(x)$ on a) and approximated c_h on b),c),d) after computing $q_{n,k}; n = 2,3,6$, where n is number of the computed function q.

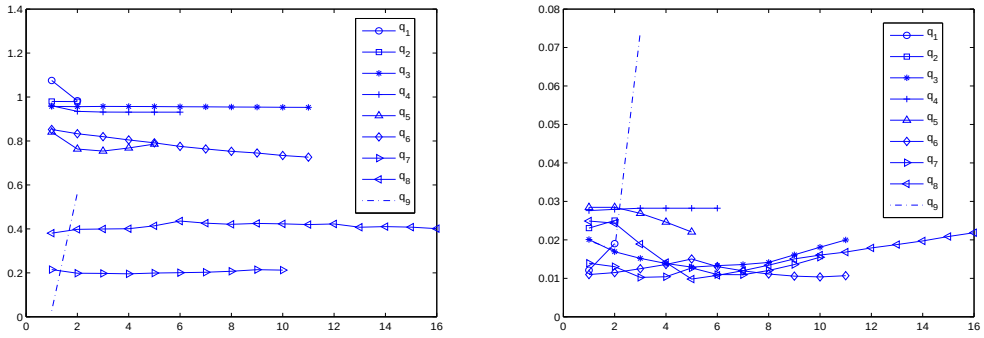

a) b)

Fig. 4 Test 1. Computed L_2-norms: on a) of the $\frac{||q_{n,i}|_{\partial\Omega} - \overline{\psi}_n||_{L_2(\partial\Omega)}}{||\overline{\psi}_n||_{L_2(\partial\Omega)}}$; on b) of the $\frac{||\tilde{V}_{n,i}|_{\partial\Omega} - \tilde{V}_n||_{L_2(\partial\Omega)}}{||\tilde{V}_n||_{L_2(\partial\Omega)}}$.

ferent values n and k shows that the inclusion/background contrasts grow with the grow of n and k. One can see from Figure 3 that the $3.1:1$ contrast in the right square is imaged for $n := \overline{N} = 7$ (see below for this choice of $\overline{N}$). As to the left square, we got the same contrast. However, location of the left square is shifted downwards, and both imaged squares are on about the same horizontal level. Values of the function $c(x) = 1$ outside of these squares are also imaged accurately though values of the function with amplitude $A = 0.5$ are cutted by cut-off regularization function.

Using Figure 4-a) which shows computed L_2-norms $F_{n,i}$, we analyze results of the reconstruction. We observe that the computed $F_{n,i}$ decrease until computing the function q_7 and on this iteration the norms are stabilized. For $n = 8,9,10$ norms $F_{n,i}$ grow steeply. Thus, we conclude, that $\overline{N} = 7$ and we take $c_{7,9}$ as our final reconstruction result. Figure 4-b) presents computed relative L_2-norms of functions $\frac{||\tilde{V}_{n,i}|_{\partial\Omega} - \tilde{V}_n||_{L_2(\partial\Omega)}}{||\tilde{V}_n||_{L_2(\partial\Omega)}}$. Using Figure 4-b) we observe that these norms have similar behavior, as in Figure 4-a).

6.3 The synthesis of the globally convergent algorithm with the adaptivity. Test 2

We take the starting point for the adaptivity computed value $c_{7,9}$ - the image obtained by the globally convergent method on the coarse mesh, which corresponds to Figure 3-d). In our tests let Γ be the side of the square Ω, opposite to the side from which the plane wave is launched and $\Gamma_T = \Gamma \times (0,T)$. In some sense the side Γ_T is the most sensitive one to the resulting data.

The adaptive algorithm means that on each mesh we minimize the functional $E_\alpha(c)$ in (19) via computing an approximate solution of the equation $E'_\alpha(c) = 0$, where $E'_\alpha(c)$ is given in (24). To do so, we use and adaptive algorithm of section 5.

On all refined meshes we have used a cut-off parameter C_{cut} for the reconstructed coefficient c_h such that

$$c_h = \begin{cases} c_h, \text{ if } |c_h - c_{glob}| \geq C_{cut} \\ c_{glob}, \text{ elsewhere.} \end{cases}$$

We choose C_{cut} different on every mesh and every quasi-Newton iteration. Here, m is the number of iterations in quasi-Newton method. Hence, the cut-off parameter ensures that we do not go too far from c_{glob}. The application of the adaptivity technique allows us to get more correct locations of both small squares depicted in Figure 5.

In the adaptive algorithm we can use box constrains for the reconstructed coefficient. We obtain these constraints using the solution obtained in the globally convergent part. Thus, in all adaptive we enforce that the coefficient $c(x)$ belongs to the set of admissible parameters, $c(x) \in C_M = \{c \in C(\overline{\Omega}) | 1 \leq c(x) \leq 4.0\}$.

We have performed numerical experiments with different noise level σ in the function $g(x,t)$ and different regularization parameters in an adaptive procedure.

opt.it.	4608	4774 elements	5272 elements	6162 elements	7622 elements	7724 elements
1	0.0124236	0.012435	0.0122961	0.0122447	0.012033	0.0122645
2	0.0137414	0.0126863	0.014033	0.0137795	0.0139721	0.0131978
3	0.0235883	0.0122284	0.0135201	0.0127081	0.0124145	0.0122671
4		0.0123446	0.0135561	0.00857489	0.012117	0.0121169
5		0.0132789			0.00503188	0.00513259
6		0.013013			0.005779	

Table 1 Test 2: $||u|_{\Gamma_T} - g||_{L_2(\Gamma_T)}$ on adaptively refined meshes. The number of stored corrections in quasi-Newton method is $n = 3$. Computations was performed with the noise level $\sigma = 0\%$ and with the regularization parameter $\gamma = 0.01$.

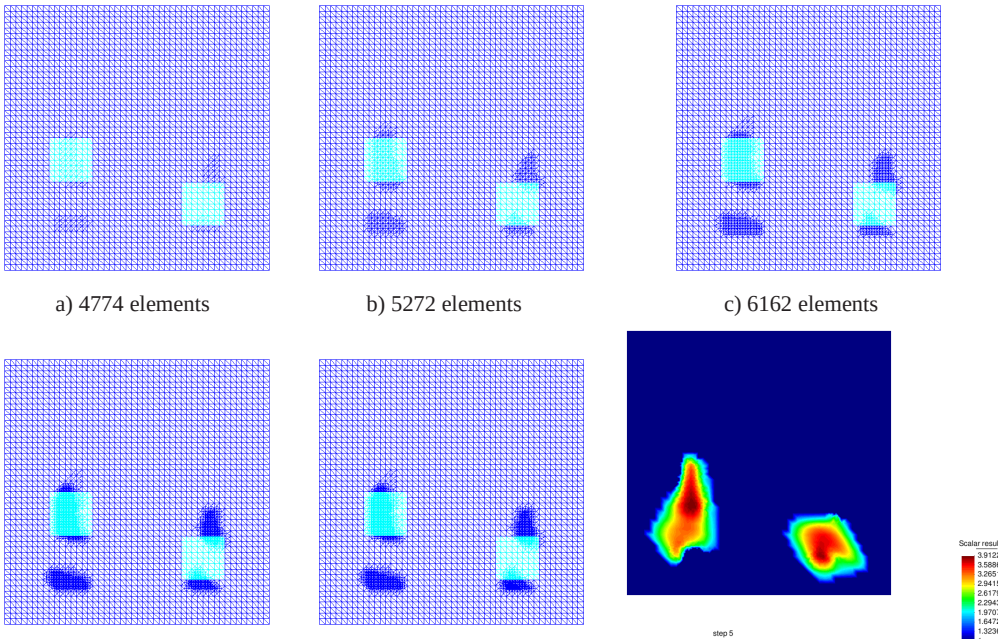

a) 4774 elements b) 5272 elements c) 6162 elements

d) 7622 elements e) 7724 elements f) $c_{h\alpha} \approx 3.91$

Fig. 5 Test 2. Computational results with $\sigma = 0\%$ and $\gamma = 0.01$. Adaptively refined computational meshes on a)-e) and spatial distribution of the parameter c_h, which corresponds to the mesh e).

We choose following values of parameters:

$$\sigma = 0\%, \alpha = 0.01, , n = 1, ..., 5;$$
$$\sigma = 1\%, \alpha = 0.01, , n = 1, ..., 5;$$
$$\sigma = 2\%, \alpha = 0.02, , n = 1, ..., 4;$$

Testing was done on 5 times adaptively refined meshes for $\sigma = 0\%, 1\%$ shown on Figures 5-a)-e),6-a)-e), and on 4 times adaptively refined mesh shown on Figure

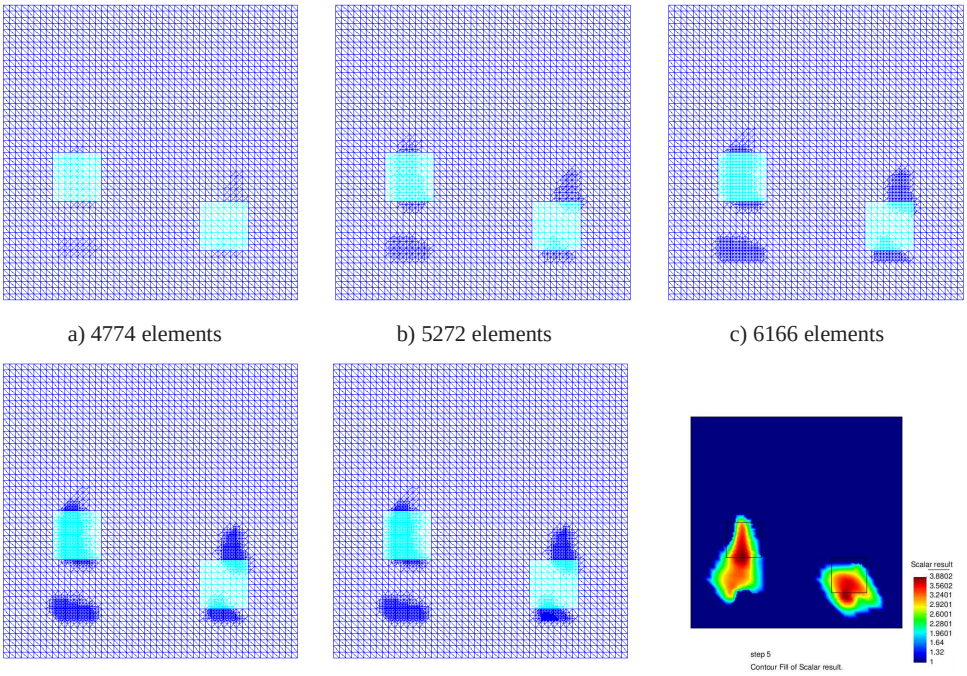

a) 4774 elements b) 5272 elements c) 6166 elements

d) 7640 elements e) 7742 elements f) $c_{h\alpha} \approx 3.88$

Fig. 6 Test 2. Computational results with $\sigma = 1\%$ and $\gamma = 0.01$. Adaptively refined computational meshes on a)-e) and spatial distribution of the parameter c_h, which corresponds to the mesh e).

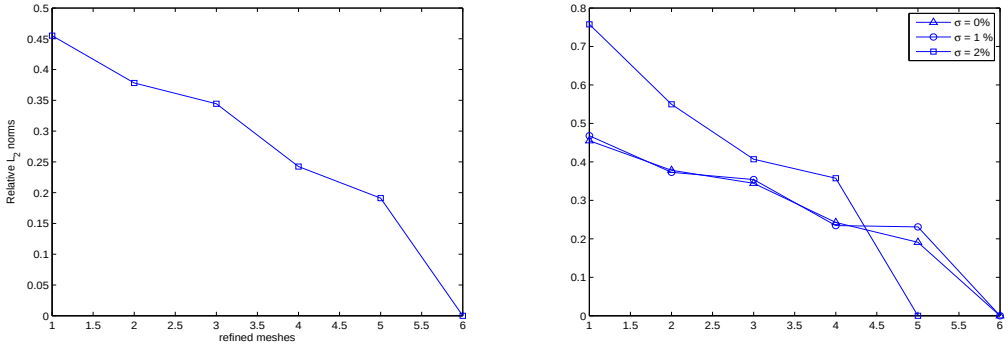

a) b)

Fig. 7 Test 2. Computed relaxation property $||c_{n+1} - c_\alpha||_{L_2} \leq q_n||c_n - c_\alpha||_{L_2}$: on a) for noise level $\sigma = 0\%$ and $\alpha = 0.01$; on b) comparison of relaxation property for different noise levels σ and different regularization parameters: $\sigma = 0\%, \alpha = 0.01, n = 1, ..., 5; \sigma = 1\%, \alpha = 0.01, n = 1, ..., 5; \sigma = 2\%, \alpha = 0.02, n = 1, ..., 4$.

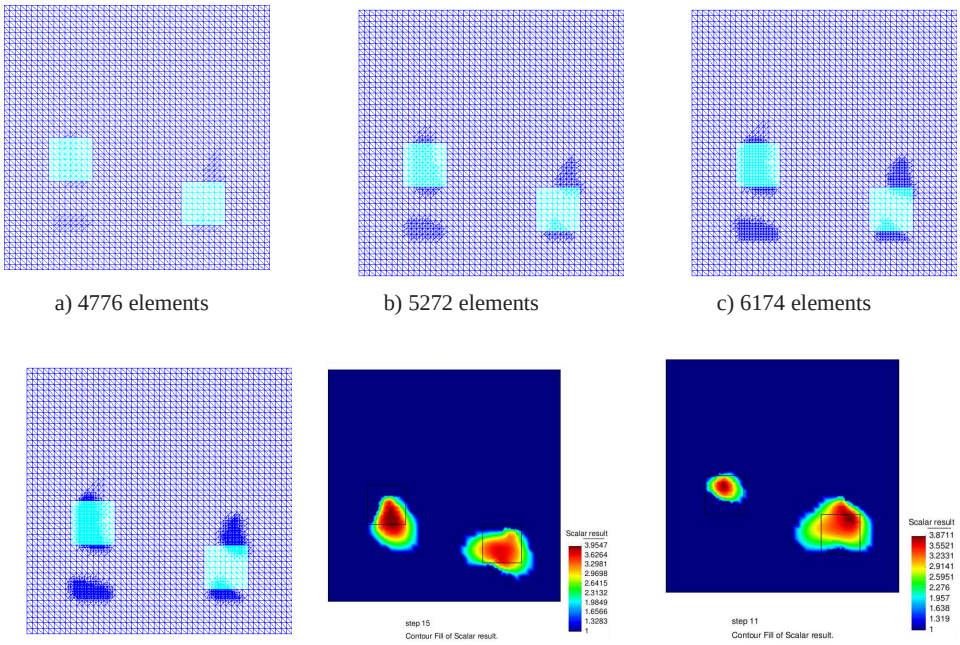

a) 4776 elements b) 5272 elements c) 6174 elements

d) 7682 elements e) $c_{h\alpha} \approx 3.9, n = 4$ f) $c_{h\alpha} \approx 3.87, n = 5$

Fig. 8 Test 2. Computational results with $\sigma = 2\%$ and $\gamma = 0.02$. Adaptively refined computational meshes on a)-d) and spatial distribution of the parameter c_{h_α} on e) for $n = 4$ and on f) for $n = 5$.

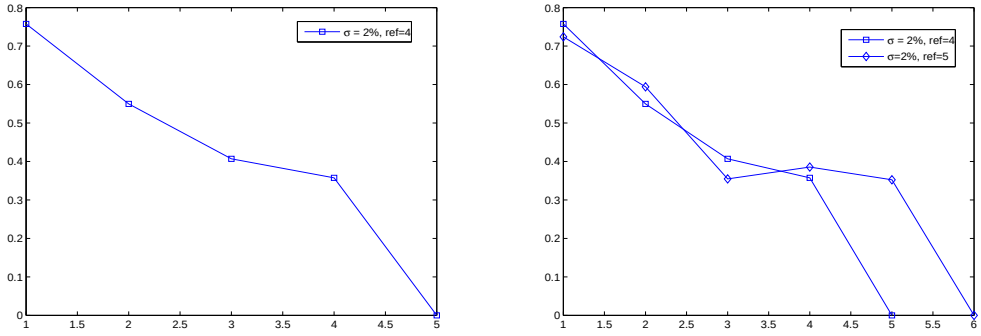

a) b)

Fig. 9 Test 2. a) Computed relaxation property $||c_{n+1} - c_\alpha||_{L_2} \leq q_n ||c_n - c_\alpha||_{L_2}$ for noise level $\sigma = 2\%$ and $\alpha = 0.02$; b) comparison of relaxation property for different c_α (different final numbers of refinement of the initial mesh).

8-a)-e). All Figures shows that the adaptivity technique enhances the quality of the reconstruction obtained on the first stage. We are able to reconstruct well locations of both small squares while values of the function around these squares are still not reconstructed. The value of the coefficient $c(x) = 1$ outside of small squares is also imaged well.

Table 1 presents computed L_2-norms of $||u|_{\Gamma_T} - g||_{L_2(\Gamma_T)}$ for $\sigma = 0\%, \alpha = 0.01$. We observe that norms at the boundary are decreasing as meshes are refined. Then they slightly increase and are finally stabilized for all refinements $n > 3$ of the initial mesh.

Figure 7 presents computed relaxation property $||c_{h_{n+1}} - c_\alpha||_{L_2} \leq q_n ||c_{h_n} - c_\alpha||_{L_2}$ between the approximated value of c_h and value of c_α taken on finally refined mesh. We take c_α on 5 times refined mesh in tests for $\sigma = 0\%, \alpha = 0.01$ and for $\sigma = 1\%, \alpha = 0.01$. When reconstructing coefficient with $\sigma = 2\%, \alpha = 0.02$ it turned out that reconstruction on 4 times refined mesh gives better results than on 5 times refined mesh.

Figure 9 shows comparison of the relaxation property for c_α after 4 refinements (see Figure 8-e) for c_α when $n = 4$) and 5 refinements (see Figure 8-f) for c_α when $n = 5$) of the initial mesh. We observe relaxation property on Figure 9-a) for $n = 4$. Thus, we take final reconstruction c_α on 4 times refined mesh in the test for $\sigma = 2\%, \alpha = 0.02$.

Acknowledgments

This research was supported by US Army Research Laboratory and US Army Research Office grant W911NF-11-1-0399, the Swedish Research Council, the Swedish Foundation for Strategic Research (SSF) in Gothenburg Mathematical Modelling Centre (GMMC) and by the Swedish Institute, Visby Program.

References

1. M. Asadzadeh and L. Beilina, *A posteriori* error analysis in a globally convergent numerical method for a hyperbolic coefficient inverse problem, *Inverse Problems*, 26, 115007, 2010.
2. A.B. Bakushinskii and M.Yu. Kokurin, *Iterative Methods for Approximate Solution of Inverse Problems*, Springer, New York, 2004.
3. W. Bangerth and A. Joshi, Adaptive finite element methods for the solution of inverse problems in optical tomography, *Inverse Problems* 24, 034011, 2008.
4. R. Becker and R. Rannacher, An optimal control approach to *a posteriori* error estimation in finite element method, *Acta Numerica*, 10, 1-102, 2001.
5. L. Beilina, K. Samuelsson and K. Åhlander, Efficiency of a hybrid method for the wave equation. In *International Conference on Finite Element Methods*, Gakuto International Series Mathematical Sciences and Applications. Gakkotosho CO., LTD, 2001.
6. L. Beilina and C. Johnson, A hybrid FEM/FDM method for an inverse scattering problem. In *Numerical Mathematics and Advanced Applications - ENUMATH 2001*, Springer-Verlag, Berlin, 2001.

7. L. Beilina, Adaptive finite element/difference method for inverse elastic scattering waves, *Applied and Computational Mathematics*, 1, 158-174, 2002.
8. L.Beilina, Adaptive finite element/difference methods for time-dependent inverse scattering problems, PhD thesis, ISBN 91-7291-317-7, 2003.
9. L. Beilina and C. Johnson, *A posteriori* error estimation in computational inverse scattering, *Mathematical Models and Methods in Applied Sciences*, 15, 23-37, 2005.
10. L. Beilina and C. Clason, An adaptive hybrid FEM/FDM method for an inverse scattering problem in scanning acoustic microscopy, *SIAM J. Sci. Comp.*, 28, 382-402, 2006.
11. L. Beilina, Adaptive finite element method for a coefficient inverse problem for the Maxwell's system, *Applicable Analysis*, 90, 1461-1479, 2011.
12. L. Beilina and M.V. Klibanov, *Approximate Global Convergence and Adaptivity for Coefficient Inverse Problems*, Springer, New York, 2012.
13. L. Beilina and M.V. Klibanov, Synthesis of global convergence and adaptivity for a hyperbolic coefficient inverse problem in 3D, *J. Inverse and Ill-posed Problems*, 18**,** 85-132, 2010.
14. L. Beilina and M.V. Klibanov, *A posteriori* error estimates for the adaptivity technique for the Tikhonov functional and global convergence for a coefficient inverse problem, *Inverse Problems*, 26**,** 045012, 2010.
15. L. Beilina and M.V.Klibanov, Reconstruction of dielectrics from experimental data via a hybrid globally convergent/adaptive inverse algorithm, *Inverse Problems*, 26, 125009, 2010.
16. L. Beilina and M.V.Klibanov, Relaxation property of the adaptivity technique for some ill-posed problems, preprint, Department of Mathematical Sciences, Chalmers University of Technology and Göteborg University, ISSN 1652-9715; nr 2012:4.
17. L. Beilina, M.V. Klibanov and M.Yu Kokurin, Adaptivity with relaxation for ill-posed problems and global convergence for a coefficient inverse problem, *Journal of Mathematical Sciences*, 167, 279-325, 2010.
18. A.L. Bukhgeim and M.V. Klibanov, Uniqueness in the large of a class of multidimensional inverse problems, *Soviet Math. Doklady*, 17, 244-247, 1981.
19. A.L. Bukhgeim, Carleman estimates for Volterra operators and uniqueness of inverse problems, in *Non-Classical Problems of Mathematical Physics*, pages 54-64, published by Computing Center of the Siberian Branch of USSR Academy of Science, Novosibirsk, 1981 (in Russian).
20. A.L. Bukhgeim, *Introduction In The Theory of Inverse Problems*, VSP, Utrecht, The Netherlands, 2000.
21. K. Eriksson, D. Estep and C. Johnson, *Calculus in Several Dimensions*, Springer, Berlin, 2004.
22. T. Feng, N. Yan and W. Liu, Adaptive finite element methods for the identification of distributed parameters in elliptic equation, *Advances in Computational Mathematics*, 29, 27-53, 2008.
23. R. Fletcher, *Practical methods of optimization*, John Wiley and Soms, Ltd, 1986.
24. A. Griesbaum, B. Kaltenbacher and B. Vexler, Efficient computation of the Tikhonov regularization parameter by goal-oriented adaptive discretization, *Inverse Problems*, 24, 025025, 2008.
25. B. Kaltenbacher, A. Krichner and B. Vexler, Adaptive discretizations for the choice of a Tikhonov regularization parameter in nonlinear inverse problems, *Inverse Problems*, 27, 125008, 2011.
26. B. Kaltenbacher, A. Neubauer and O. Scherzer, *Iterative Regularization Methods for Nonlinear Ill-Posed Problems*, de Gruyter, New York, 2008.
27. M. V. Klibanov, Uniqueness of solutions in the 'large' of some multidimensional inverse problems, in *Non-Classical Problems of Mathematical Physics*, pages 101-114, 1981, published by Computing Center of the Siberian Branch of the USSR Academy of Science, Novosibirsk (in Russian).
28. M. V. Klibanov, Inverse problems in the 'large' and Carleman bounds, *Differential Equations*, 20, 755-760, 1984.
29. M. V. Klibanov, Inverse problems and Carleman estimates, *Inverse Problems*, 8, 575–596, 1992.

30. M. V. Klibanov and A. Timonov, *Carleman Estimates for Coefficient Inverse Problems and Numerical Applications*, VSP, Utrecht, 2004.
31. M. V. Klibanov, M. A. Fiddy, L. Beilina, N. Pantong and J. Schenk, Picosecond scale experimental verification of a globally convergent numerical method for a coefficient inverse problem, *Inverse Problems*, 26, 045003, 2010.
32. N.A. Koshev, L. Beilina, A posteriori error estimates for the Fredholm integral equation of the first kind, accepted to book series *Springer Proceedings in Mathematics*, 2012.
33. A.V. Kuzhuget, L. Beilina, M.V. Klibanov, A. Sullivan, L. Nguyen and M.A. Fiddy, Blind experimental data collected in the field and an approximately globally convergent inverse algorithm, preprint, available online at http://www.ma.utexas.edu/mp_arc/.
34. O. A. Ladyzhenskaya, *Boundary Value Problems of Mathematical Physics*, Springer Verlag, Berlin, 1985.
35. J. Li, J. Xie and J. Zou, An adaptive finite element reconstruction of distributed fluxes, *Inverse Problems*, 27, 075009, 2011.
36. J. Nocedal, Updating quasi-Newton matrices with limited storage, *Mathematics of Comp.*, V.35, N.151, 773–782, 1991.
37. J.R. Reitz, F.J. Milford, and R.W. Christy, *Foundations of Electromagnetic Theory*, Reading, Mass.: Addison-Wesley, 1980.
38. A. N. Tikhonov and V. Ya. Arsenin, *Solutions of Ill-Posed Problems*, Winston and Sons, Washington, DC, 1977.
39. A.N. Tikhonov, A.V. Goncharsky, V.V. Stepanov and A.G. Yagola, *Numerical Methods for the Solution of Ill-Posed Problems*, London: Kluwer, London, 1995.
40. A. N. Tikhonov and A.A. Samarskii, *Equations of Mathematical Physics (Dover Books on Physics)*, New York: Dover Publications, Inc., 1990.
41. WavES at http://www.waves24.com/